Mathematical Biosciences and Engineering

MBE, 18(6): 9806–9821.
DOI: 10.3934/mbe.2021481
Received: 31 July 2021
Accepted: 21 October 2021
Published: 05 November 2021

http://www.aimspress.com/journal/MBE

Research article

Construction of competitive endogenous RNA network related to circular RNA and prognostic nomogram model in lung adenocarcinoma

Pingping Song[1], Jing Chen[2], Xu Zhang[1,*] and Xiaofeng Yin[1]

[1] School of Mathematics and Statistics, Southwest University, Chongqing 400715, China
[2] School of Science, Southwest University of Science and Technology, Sichuan 621000, China

* **Correspondence:** Email: zhangxu1107@163.com.

Abstract: Early researches have revealed that circular RNA (circRNA) had the potential of biomarkers and could affect tumor progression through regulatory networks. However, few research focused on the function of circRNA in lung adenocarcinoma and the regulation mechanism of competitive endogenous RNA. In present study, through differential expression analysis, 10 circRNAs, 98 miRNAs(microRNA) and 2497 mRNAs were screened. Based on the 10 circRNAs and related databases, a competitive endogenous RNA regulatory network (ceRNA network) containing 7 circRNAs, 13 miRNAs and 147 mRNAs was constructed. KEGG and GO analysis suggested that 147 mRNAs were obviously enriched in biological pathway related to LUAD. By constructing a PPI network, 12 hub genes were identified by MCODE. The result of survival analysis showed that 10 hub genes (BIRC5, MKI67, CENPF, RRM2, BUB1, MELK, CEP55, CDK1, NEK2, TOP2A) were significantly related to the survival of LUAD. We randomly divided 483 clinical data into two parts: train set and validation set. The train set was used for Cox regression analysis, 3 prognostic factors (stage, T, CDK1) were screened. The nomogram model was constructed based on stage, T and CDK1. The model was evaluated by ROC curve, calibration chart, Kaplan-Meier (KM) curve and validation set data. The results indicated that the model has good accuracy. Our study elucidated the regulatory mechanism of circRNA in lung adenocarcinoma, and the nomogram model also provided insight for the clinical analysis of lung adenocarcinoma.

Keywords: lung adenocarcinoma; circular RNA; competitive endogenous network; nomogram model; bioinformatics

1. Introduction

There are many kinds of malignant tumors, but lung cancer is the most common one. It mainly causes cancer morbidity and death, causing 18.4% of the cancer deaths [1]. There are many types of lung cancer, of which lung adenocarcinoma (LUAD) is the most common, which is often caused by tumor cell driven oncogene aberrations [2]. Notably, the incidence rate of LUAD significantly raised and it constituted nearly 40% of the incidence of all lung malignancies [3]. Although experts have made headway in therapy and diagnosis, the survival rate in 5 years of patients with LUAD is less than 20% due to its complex mechanism [4]. Therefore, understanding the potential regulatory mechanism of LUAD, looking for new biomarkers and establishing an effective prognostic nomogram model are essential for the prognosis and treatment of LUAD.

In 2011, Salmmena et al. put forward the hypothesis of competitive endogenous RNA (ceRNA), believing that noncoding RNA could indirectly regulate mRNA expression by competitively binding miRNA [5]. CircRNA is a new noncoding RNA molecule with complete closed-cycle structure [6]. Unlike linear RNAs that are terminated with 5' caps and 3' tails, circRNA is not affected by RNA exonuclease and its expression is more stable [7]. Studies have shown that circRNA could affect the generation and evolution of tumors. For example, studies have reported that circRNA plays a pivotal role in the pathogenesis of lung cancer and hold important clinical relevance [8]. CircRNA can participate in the proliferation, invasion, metastasis and apoptosis of gastric cancer [9]. CircRNA expression has an extensive effect on the biological behavior of hepatocellular carcinoma [10]. Numerous researches have indicated that circRNA is enriched and stable in exosomes and can be taken as biomarkers of cancer [11–13]. Recently, it has been found that circRNA is abundant in miRNA connection sites and can play the part of miRNA sponges, which makes circRNA become hot point in research of ceRNA family. CircRNA can indirectly influence the steadiness or translation of targeted mRNA by the way of competing with miRNA, thereby regulating gene expression [14]. For example, CiRS-7 could promote the metastasis and development of oral squamous cell carcinoma through the RAF-1/PIK3CD pathway [15]; circRNA hsa_circ_0012673 promoted the proliferation of lung adenocarcinoma by interacting with miR-22 [16]. Circ_0001588 promoted the malignant progression of lung adenocarcinoma by binding miR-524-3p to /NACC1 signaling [17]. Previous studies have reported the possible existence of ceRNA network in LUAD. For example, Liang et al. constructed ceRNA network associated with hsa_circ_0072088 and has_circ_0008274 [18]; Liu et al. suggested that hsa_circ_0005962 and hsa_circ_0086414 might be biomarkers of LUAD [19]. However, the research on circRNA and its ceRNA network in lung adenocarcinoma is still insufficient. Many circRNAs and related ceRNA network still need to be discovered.

In present study, circRNAs, miRNAs and mRNAs with abnormally expression in cancer and normal samples were extracted by differential analysis. Then, by pairwise predicting, a circRNA-miRNA-mRNA network was structured. The GO and KEGG enrichment analysis were carried out to understand the latent biological functions of mRNAs. Hub gene was screened by MCODE from PPI network. Verified by survival analysis, circRNA-miRNA-hub gene subnetwork was structured. Cox regression analysis was used to filter factors related to survival rate of LUAD. With the prognostic factors, a prognostic nomogram model for patients with LUAD was constructed and verified.

2. Materials and methods

2.1. Data collection

CircRNA data of LUAD were acquired from the Gene Expression Omnibus (GEO, https://www.ncbi.nlm.nih.gov/geo/), and two datasets GSE101586 (5 cancerous samples, 5 normal samples) and GSE101684 (4 cancerous samples, 4 normal samples) were selected. The expression matrices of the two datasets were combined by taking the intersection with respect to the name of circRNAs. The Combat function in the sva package was used to eliminate the batch effects according to the number of samples in the control group and the experimental group in the two datasets. The Cancer Genome Atlas (TCGA) database (https://xenabrowser.net, updated by the end of April, 2020) is a database for acquiring gene expression data where we obtained miRNA expression data (518 cancerous samples, 46 normal samples) and mRNA expression data (526 cancerous samples, 59 normal samples). Clinical data (age, gender, stage, T, N, OS time and OS) were also download from TCGA database (513 patient samples). A total of 483 patient samples were retained after deleting the samples with missing clinical characteristics.

2.2. Differential expression analysis of three kinds of RNA

Based on the combined dataset after batch effect normalization, the expression file of circRNA were further analyzed to obtain differentially expressed circRNA (DEcircRNA) by using the limma package. The screening thresholds were $P < 0.01$ and $|\log2FC| > 2$. The differentially expressed miRNAs (DEmiRNAs) and differentially expressed mRNAs (DEmRNAs) were screened through the edgeR package. The screening thresholds were False-Discovery Rate < 0.05 and $|\log2(FC)| > 2$.

2.3. Construction of circRNA-associated ceRNA network

Cancer-Specific CircRNA Database (CSCD) [20] (http://gb.whu.edu.cn/CSCD/) is a database for studying of tumor specific circRNA, from which we can predict the target miRNA of circRNA. The predicted miRNA and DEmiRNA were crossed, and the ceRNA network was constructed using the miRNA shared by the two datasets.

Using miRTarbase [21] (http://mirtarbase.mbc.nctu.edu.tw/) and Targetscan [22] (http://www.targetscan.org/) to collect the target mRNA of miRNA. Only mRNAs that existed in two databases were finally selected. The predicted mRNA and DEmRNA were crossed, and the ceRNA network was constructed using the mRNA shared by the two datasets.

Finally, the ceRNA network associated with circRNA was identified through the miRNA-circRNA and miRNA-mRNA relationship pairs. The ceRNA regulatory network was visualized by Cytoscape 3.7.0 software (http://www.cytoscape.org/) [23].

2.4. Functional enrichment analysis of mRNAs

For exploring the latent biological mechanism and functions of mRNAs in the ceRNA network, the DAVID database [24,25] (https://david.ncifcrf.gov/)was used to perform GO function enrichment analysis and KEGG pathway enrichment analysis. The results of enrichment analysis were visualized by ggpolt2 R package.

2.5. Construction of PPI network and screening of hub genes

To further study the interaction among mRNAs in the ceRNA network, PPI network was analyzed by Search Tool for the Retrieval of Interacting Genes [26] (STRING, version 11, https://string-db.org/) database. The STRING database has a combined score for each PPI relationship pair that is distributed between 0 and 1. The higher the total score, the more reliable the PPI relationship. In current study, we chose combined score greater than 0.9 as the threshold. Then, the Molecular Complex Detection (MCODE), a clustering algorithm identifying densely connected regions of a molecular interaction network [27], was used to screen modules of hub genes from the PPI network.

2.6. Survival analysis of hub genes

GEPIA [28] (http://gepia.cancer-pku.cn/) integrated gene expression data from GTEX and TCGA projects which can be used for multiple data analysis and visualization. The prognostic value of hub genes in LUAD were analyzed by survival analysis tool in GEPIA. UALCAN (http://ualcan.path.uab.edu/index.html) [29] is a web resource for analyzing cancer transcriptome data based on TCGA database, which can perform biomarker identification, expression spectrum analysis, survival analysis and so on. To ensure the accuracy of the results, we further verified the prognostic value of hub gene in TCGA (through the survival analysis package in R software) and the UALCAN database. Then, based on the hub genes with prognostic value, circRNA-miRNA-hub gene subnetwork was identified to explore important regulatory module in the ceRNA network.

2.7. Screening of prognostic factors by Cox regression analysis

According to the proportion of 7:3, all LUAD samples were randomly chopped into train set and validation set. Fisher exact test and wilcox test were used to test whether there was significant difference between two datasets. Univariate Cox regression analysis of the train set was performed using Survival package of R software to identify the factors significantly associated with the survival of LUAD. In the univariate Cox analysis, the factors with p value < 0.05 were further included in multivariate Cox regression analysis. Multivariate Cox regression analysis was used to screen independent prognostic factors, and hazard ratio (HRS) and regression coefficient were calculated.

2.8. Construction and validation of nomogram model

Based on the prognostic factors, the nomogram model was established by rms package of R software. In the nomogram model, we first set the scoring standard according to the regression coefficient of each influence factor, and then give the score value of each influence factor, thereby calculating the total score of each patient [30]. Finally, the conversion between the probability of occurrence and the total score is calculated by a function to evaluate the 1-year, 3-year and 5-year OS of LUAD patients. The ROC curves of train set and validation set were drawn by survivalROC package, and the differentiation of the model was assessed by calculating the area under ROC curve (AUC). Calibration chart of train set and validation set was used to evaluate the calibration degree of the model by comparing the difference between prediction probability and survival probability of nomogram model. Considering the median of the total scores as the cut-off value, the LUAD samples were divided

into high risk group and low risk group. Then, we analyzed the evaluation ability of the model for high risk and low risk populations through survival analysis.

3. Results

3.1. Differential expression analysis of three kinds of RNA

A total of 10 DEcircRNAs were obtained in the merged dataset (4 up-regulated, 6 down-regulated). From the TCGA database, 98 DEmiRNAs (79 up-regulated, 19 down-regulated) and 2497 DEmRNAs (1983 up-regulated, 514 down-regulated) were screened.

3.2. Construction of circRNA-associated ceRNA network

The CSCD database was utilized to find targeted miRNAs of 10 DEcircRNAs. 466 circRNA-miRNA relationship pairs (9 circRNAs, 423 miRNAs) were acquired. After crossing with 98 DEmiRNAs, 19 circRNA-miRNA relationship pairs (7 circRNAs, 13 miRNAs) were identified. 13 miRNA-related mRNAs were collected by miRTabase and Targetscan. The results of the two databases were intersected, 2532 miRNA-mRNA relationship pairs were obtained. After crossing with 2497 DEmRNAs, 177 miRNA-mRNA relationship pairs (13 miRNAs, 147 mRNAs) were acquired. Through the final circRNA-miRNA and miRNA-mRNA relationship pairs, the circRNA-miRNA-mRNA regulatory network was determined，including 7 circRNAs, 13 miRNAs and 147 mRNAs (Supplementary Table 1). Ultimately, the ceRNA regulatory network was drew by Cytoscape software (Figure 1).

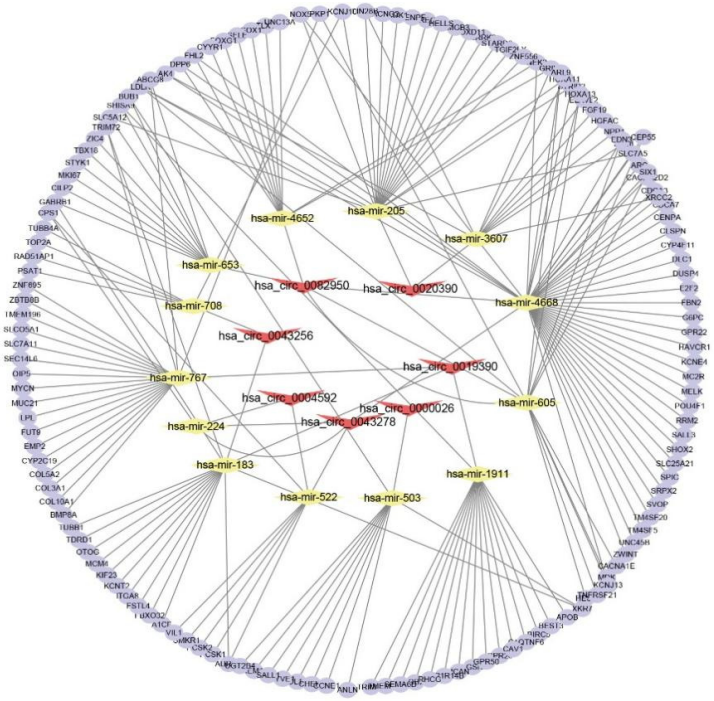

Figure 1. The ceRNA network of 7 circRNAs, 13miRNAs and 147 mRNAs. The red represents circRNA, yellow represents miRNAs, and purple represents mRNAs.

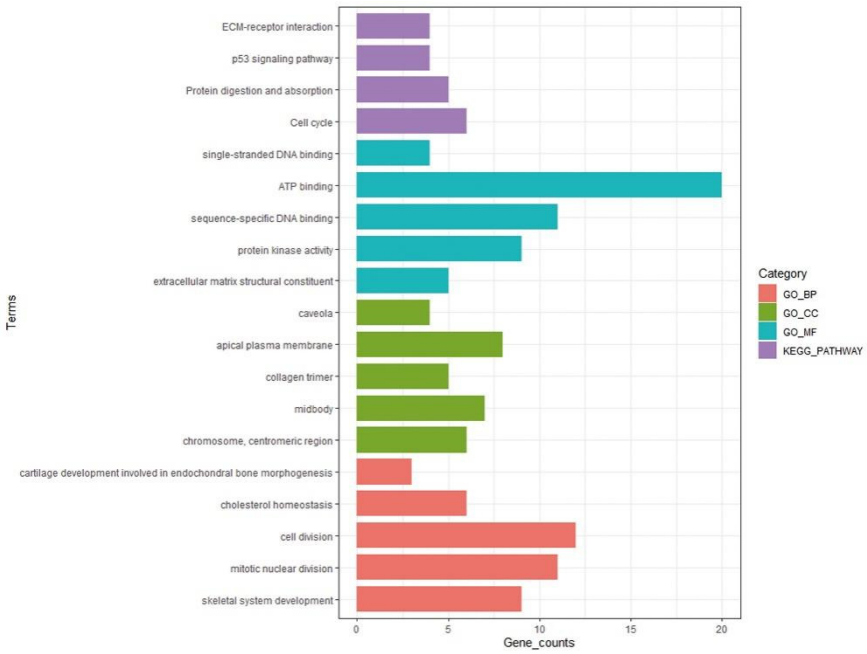

Figure 2. KEGG and GO enrichment analysis of 147 mRNAs.

3.3. Enrichment analysis of mRNAs

GO and KEGG analysis were applied to explore the functions of the 147 mRNAs. KEGG enrichment analysis identified 4 KEGG pathways and GO enrichment analysis identified 58 GO Terms. The results of 4 KEGG pathways and top 15 Go terms (5 biological processes, 5 cell components and 5 molecular functions) were shown in Figure 2. As can be known from Figure 2 that the most enriched KEGG pathway terms were correlated with ECM-receptor interaction, cell cycle, protein digestion and absorption and p53 signaling pathway. The most enriched GO terms were correlated with single-stranded DNA binding, ATP binding, sequence-specific DNA binding, protein kinase activity, extracellular matrix structural constituent, caveola, apical plasma membrane, collagen trimer, midbody, chromosome and centromeric region, cartilage development involved in endochondral bone morphogenesis, cholesterol homeostasis, cell division, mitotic nuclear division and skeletal system development.

3.4. Construction of PPI network and screening of hub genes

To further explore the relationship among mRNAs, PPI network was constructed by Cytoscape software which contained 39 nodes and 230 edges. A total of 12 hub genes (BIRC5, MKI67, CENPF, AURKA, KIF23, RRM2, BUB1, MELK, CEP55, CDK1, NEK2 and TOP2A) were screened by MCODE plugin from the PPI network (Figure 3).

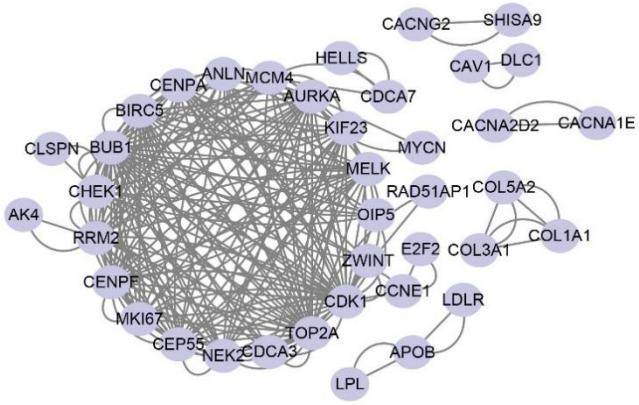

Figure 3. PPI network diagram of 147 mRNA.

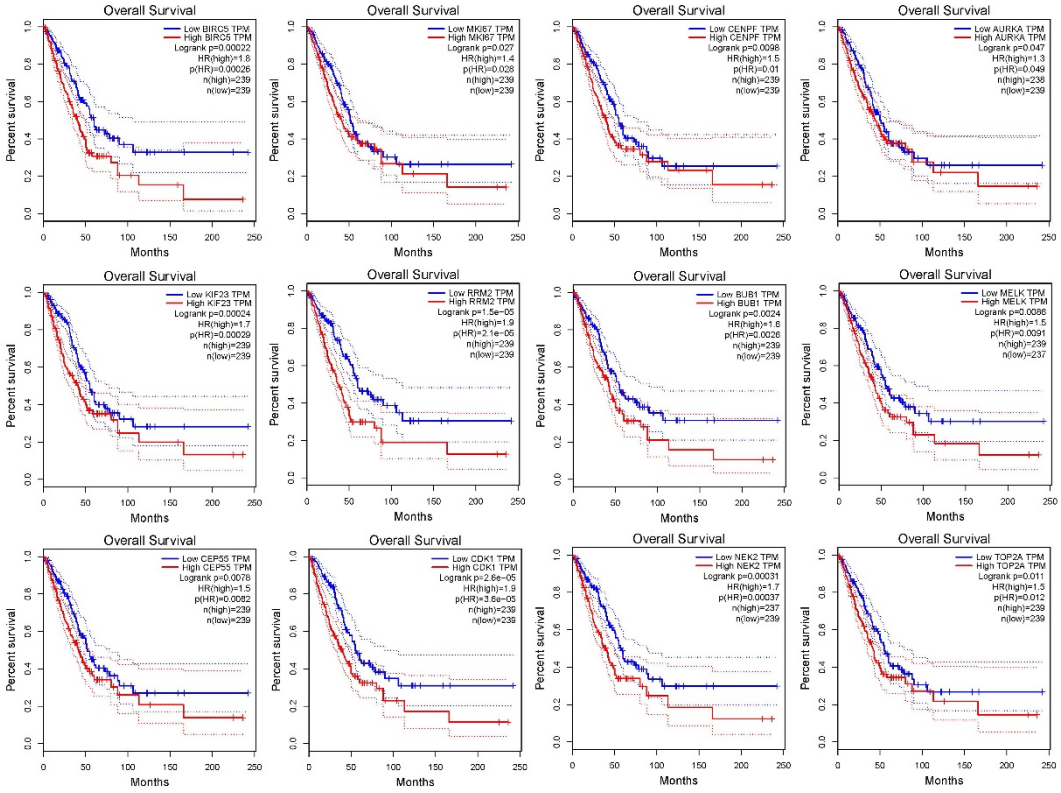

Figure 4. Survival analysis of 12 hub genes.

3.5. Survival analysis of 10 hub genes

GEPIA analysis results showed that 12 hub genes were closely related with the survival of lung adenocarcinoma (Figure 4). The survival analysis result of R based on TCGA dataset indicated that 11 genes were significantly correlated with the survival of LUAD, except for AURKA (Supplementary Figure 1). The result of survival analysis in UACLAN database indicated that 11 genes were significantly associated with the survival of LUAD, except for KIF23 (Supplementary Figure 2).

Therefore, 10 genes (BIRC5, MKI67, CENPF, RRM2, BUB1, MELK, CEP55, CDK1, NEK2 and TOP2A) in the intersection of the three methods were considered as important prognostic genes for the survival of the patients with LUAD. Based on the 10 hub genes, we built circRNA-miRNA-hub gene regulation subnetwork (Figure 5).

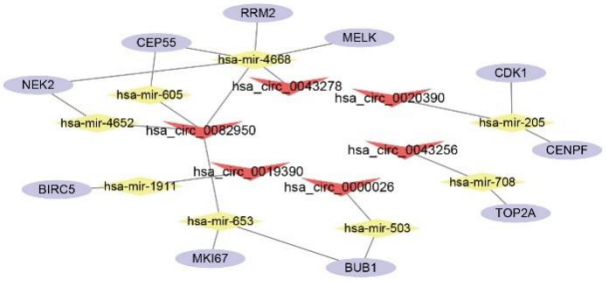

Figure 5. CircRNA-miRNA-hub gene regulation network.

3.6. Screening of prognostic factors by Cox regression analysis

The clinical characteristics and test result of LUAD samples were shown in Table1.The two datasets were not obviously different because all P values were greater than 0.05. The Cox regression analysis results of train set were shown in Table 2. Univariate analysis showed that the P values of stage, T and 9 hub genes（except for AURKA） were all less than 0.05, indicating that these variables were connected with the survival of LUAD patients. Then, we incorporated these variables into the multivariate Cox analysis and the result suggested that stage, T and CDK1 were statistically significant ($P < 0.05$), which implied these variables were independent prognostic factors.

Table 1. Clinical characteristics and test results of LUAD included in this study

Variables	Level	Patients (N = 483)	Train set (N = 338)	Validation set (N = 145)	P
Age (%)	<= 65	236 (48.9)	168 (49.7)	68(46.9)	0.62
	> 65	247 (51.1)	170 (50.3)	77 (53.1)	
Sex (%)	female	225 (46.6)	159 (47.0)	72(49.5)	0.426
	male	258 (53.4)	179 (53.0)	73 (50.3)	
Stage (%)	Stage i	265 (54.9)	185 (54.7)	67(53.7)	0.124
	Stage ii	118 (24.4)	187 (55.3)	41 (28.3)	
	Stage iii	79 (16.4)	77 (22.8)	24 (16.6)	
	Stage iv	21 (4.3)	55 (16.3)	2 (1.4)	
T (%)	T1	164 (34.0)	19 (5.6)	50(34.4)	0.142
	T2	257 (53.2)	114 (33.7)	81 (55.9)	
	T3	45 (9.3)	176 (52.1)	13 (9.0)	
	T4	17 (3.5)	32 (9.5)	1 (0.7)	
N (%)	N0	323 (66.9)	16 (4.7)	92(63.4)	0.56
	N1	90 (18.6)	231 (68.3)	30 (20.7)	
	N2 + N3	70 (14.5)	60 (17.8)	23 (15.9)	

Table 2. Univariate and multivariate Cox regression analysis results of train set.

Variables	Univariate		Multivariate	
	HR (95%CI)	P	HR (95%CI)	P
Age (<= 65/> 65)	1.010 (0.708–1.441)	0.956		
Sex(male/female)	0.819 (0.574–1.168)	0.27		
Stage i	1		1	
Stage ii	2.195 (1.399–3.445)	0.001	1.675 (0.800–3.508)	0.172
Stage iii	3.380 (2.149–5.317)	< 0.001	2.934 (0.949–9.065)	0.061
Stage iv	3.417 (1.765–6.618)	< 0.001	2.844 (1.221–6.621)	0.015
T1	1		1	
T2	4.379 (2.179–8.801）	0.098	1.107 (0.694–1.766)	0.669
T3	2.263 (1.485–3.448)	< 0.001	2.215 (1.030–4.765)	0.042
T4	2.474 (1.564–3.914)	< 0.001	1.512 (0.659–3.469)	0.330
N0	1		1	
N1	2.263 (1.485–3.448)	< 0.001	1.506 (0.746–3.043)	0.254
N2 + N3	2.474 (1.564–3.914)	< 0.001	0.941 (0.335–2.640)	0.907
BIRC5	1.146 (1.019–1.289)	0.022	0.724 (0.501–1.045)	0.084
MKI67	1.200 (1.051–1.371)	0.007	1.155 (0.719–1.854)	0.552
CENPF	1.167 (1.025–1.329)	0.019	1.140 (0.767–1.696)	0.517
RRM2	1.23 (1.079–1.403)	0.002	0.763 (0.462–1.260)	0.290
BUB1	1.182 (1.035–1.350)	0.013	0.963 (0.675–1.373)	0.834
MELK	1.168 (1.039–1.313)	0.009	0.804 (0.504–1.284)	0.361
CEP55	1.198 (1.053–1.363)	0.006	1.786 (1.088–2.930)	0.022
CDK1	1.246 (1.078–1.439)	0.003	1.218 (0.793–1.871)	0.368
NEK2	1.193 (1.055–1.348)	0.005	1.060 (0.685–1.642)	0.794
TOP2A	1.12 (0.993–1.263)	0.065		

3.7. Establishment and verification of nomogram model

On the basis of 3 prognostic factors (stage, T and CDK1), a prognostic nomogram model (Figure 6) was constructed to study the 1-year, 3-year and 5-year survival rates of LUAD. In the ROC curve of the train set (Figure 7A), the AUC value of the 1-year, 3-year and 5-year were 0.739, 0.727 and 0.665, respectively. While in that of validation set (Figure 7B), the AUC value of the 1 year, 3 year and 5 year were 0.693, 0.625 and 0.677, respectively. The results showed that the model had good discrimination. The calibration charts in train set and validation set (Figure 8) did not deviate from the ideal line. The KM survival curves (Figure 7C,D) in train set and validation set showed that the survival rate of the high risk group is obviously lower than that of the low risk group, which further verified the validity and applicability of the model.

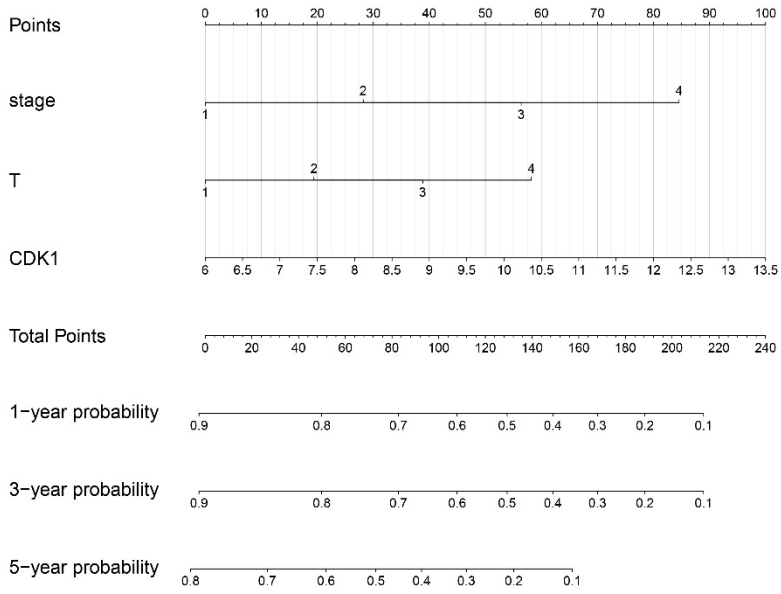

Figure 6. Nomogram models for predicting 1-year, 3-year, and 5-year overall survival rates with LUAD.

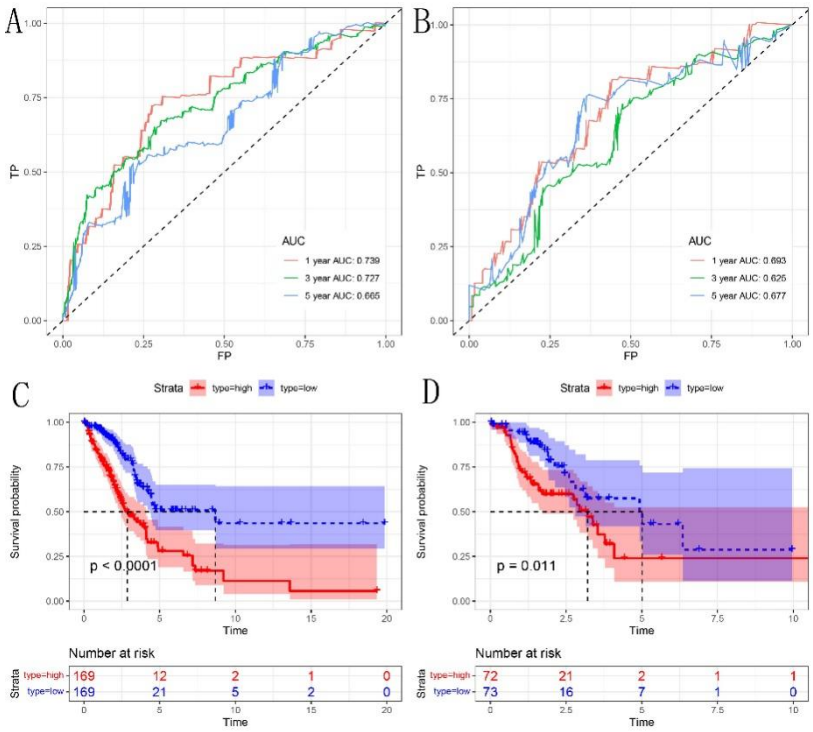

Figure 7. ROC curve (A)train set (B) validation set. The survival analysis curve of the high risk group and the low risk group (C) train set (D) validation set.

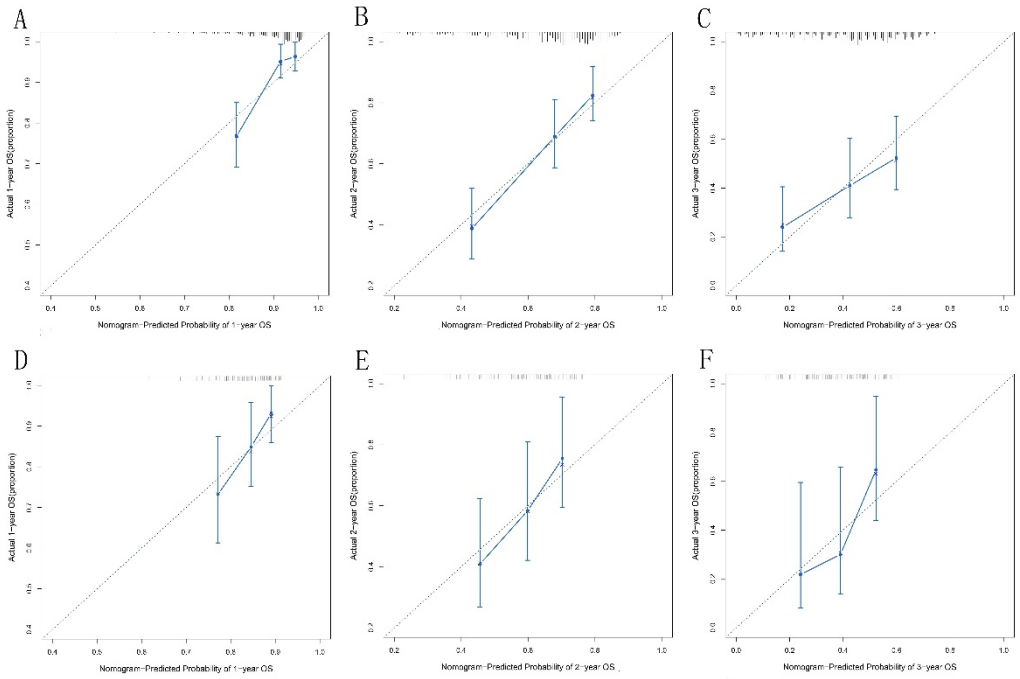

Figure 8. (A, B, C) calibration charts of 1-year, 3-year and 5-year survival rates in train set, (D, E, F) calibration charts of 1-year, 3-year and 5-year survival rates in validation set.

4. Discussion

Previous studies have shown that circular RNA could be used as biomarker of cancer, and could promote the invasion, immigration and propagation of tumor cells through regulatory mechanisms. In the current study, 10 circRNAs were extracted by differential analysis. Through the mutual analysis of various databases, a ceRNA regulatory network containing 7 circRNAs, 13 miRNAs, and 147 mRNAs was finally constructed. The 7 circRNAs were hsa_circ_0043278, hsa_circ_0043256, hsa_circ_0000026, hsa_circ_0082950, hsa_circ_0004592, hsa_circ_0020390, hsa_circ_0019390. Studies have confirmed that hsa_circ_0043278 (alias circTADA2A) could promote the proliferation and migration of non-small cell lung cancer cells by regulating the miR 638/KIAA0101 signaling pathway [31]; propofol could inhibit canceration of lung cancer cells through hsa_circ_0043278/miR-455-3p/FOXM1 axis [32]. Meanwhile, hsa_circ_0043278 has also been confirmed by experiments to play a key role in breast cancer and glioma. [33,34]. In addition, studies have reported that hsa_circ_0043256/miR-1252/ITCH axis might suppress Wnt /b-catenin pathway activities, resulting in apoptosis of non-small cell lung cancer [35]; hsa_circ_0000026(alias circ-EIF4G3) could promoted the proliferation and migration of gastric cancer via sponging miR-335[36]. Studies have also shown that hsa_circ_0020390 (alias Circ_DOCK1) could inhibit the growth and metastasis of colorectal cancer cells and increase cell apoptosis by regulating the miR-132-3p/USP11 axis [37]. However, hsa_circ_0004592, hsa_circ_0082950 and hsa_circ_0019390 have not been reported yet. Therefore, these identified circRNAs may be important circRNAs for lung adenocarcinoma. Hopefully these circRNAs could be further verified by biological experiments in future.

MiRNA is a type of single-stranded RNA molecule encoded by endogenous genes. It is known that miRNA could regulate the expression of target genes by interacting with them [38]. In this study,

we found 13 miRNAs through the ceRNA network. Most of these miRNAs have been shown to be involved in the progression of lung adenocarcinoma, non-small cell lung cancer or lung cancer. For example, overexpression of miR-183-5p might play an oncogenic role in LUAD through involvement in the regulatory networks of its target genes [39]； miR-3607 promoted LUAD proliferation by inhibiting APC expression [40]; miR-767-3p could inhibit growth and migration of LUAD cells by regulating CLDN18 [41]; miR-708 participated in tumor growth and disease progression as a tumor gene by directly down regulating Wnt signaling pathway in lung cancer [42]; miR-605 inhibited the oncogenicity of non-small-cell lung cancer by directly targeting Forkhead Box P1 [43]; miR-503 inhibited non-small-cell lung cancer by targeting PDK1/PI3K/AKT pathway [44]; LncRNA HCG11 inhibited cell viability, migration and invasion in non-small-cell lung cancer by functioning as a ceRNA of miR-522-3p to upregulate SOCS5 [45]; Circular RNA circ-RAD23B promoted cell growth and invasion by miR-653-5p/TIAM1 pathways in non-small-cell lung cancer [46]; miR-205 could act as a promising biomarker in the diagnosis and prognosis of lung cancer [47]; miR-1911-3p could interact with the targeted mEAK-7 to inhibit mTOR signal transduction in human lung cancer cells [48].

The GO and KEGG analysis results suggested that these selected mRNAs in the ceRNA network were significantly enriched in biological functions and pathways related to LUAD. For example, Chromatin patterns were associated with lung adenocarcinoma progression [49]; the score of cell cycle progression could be used as a marker of specific death risk in patients with LUAD [50]; UBE2T could promote autophagy via the p53/AMPK/mTOR signaling pathway in lung adenocarcinoma [51]; ATP binding cassette E1 could enhance viability and invasiveness of lung adenocarcinoma cells in vitro [52]; inhibitor of DNA-binding protein 4 could suppress LUAD metastasis through the regulation of epithelial mesenchymal transition [53].

5. Conclusions

In this study, we found the important circRNAs in LUAD, constructed the ceRNA regulatory network and discovered important regulatory modules, which provided potential curative targets and molecular mechanisms for LUAD. Meanwhile, a nomogram model was established to forecast the survival of LUAD, which will be helpful to the prognosis and therapy of LUAD patients.

Acknowledgments

Our deepest gratitude goes to the editors and anonymous reviewers for their careful work and thoughtful suggestions that have helped to improve this paper substantially.

This study was supported by the Natural Science Foundation of China (No.11701471 and 12071382, http://www.nsfc.gov.cn/) and Basic Science and Frontier Technology Research Project of Chongqing (cstc2017jcyjAX0476, http:/kjj.cq.gov.cn).

Conflict of interest

The authors declare no conflict of interests.

References

1. F. Bray, J. Ferlay, I. Soerjomataram, R. L. Siegel, L. A. Torre, A. Jemal, Global cancer statistics 2018: GLOBOCAN estimates of incidence and mortality worldwide for 36 cancers in 185 countries, *Ca-Cancer J. Clin.*, **68** (2018), 394–424.
2. M. Saito, K. Shiraishi, H. Kunitoh, S. Takenoshita, J. Yokota, T. Kohno, Gene aberrations for precision medicine against lung adenocarcinoma, *Cancer Sci.*, **107** (2016), 713–720.
3. H. Nakamura, H. Saji, Worldwide trend of increasing primary adenocarcinoma of the lung, *Surg. Today*, **44** (2014), 1004–1012.
4. L. Osmani, F. Askin, E. Gabrielson, Q. K. Li, Current WHO guidelines and the critical role of immunohistochemical markers in the subclassification of non-small cell lung carcinoma (NSCLC): Moving from targeted therapy to immunotherapy, *Semin. Cancer Biol.*, **68** (2017), 103–109.
5. L. Salmena, L. Poliseno, Y. Tay, L. Kats, P. Pandolfi, A ceRNA hypothesis, The Rosetta Stone of a hidden RNA language?, *Cell*, **146** (2011), 353–358.
6. S. Qu, X. Yang, X. Li, J. Wang, Y. Gao, R. Shang, et al., Circular RNA: A new star of noncoding RNAs, *Cancer Lett*., **365** (2015), 141–148.
7. W. R. Jeck, J. A. Sorrentino, K. Wang, M. K. Slevin, C. E. Burd, J. Liu, et al., Circular RNAs are abundant, conserved, and associated with ALU repeats, *RNA*, **19** (2013),141–157.
8. C. Wang, S. Tan, J. Li, W. R. Liu, Y. Peng, W. Li, CircRNAs in lung cancer-Biogenesis, function and clinical implication, *Cancer Lett.*, **492** (2020), 106–115.
9. X. W. Li, W. H. Yang, J. Xu, Circular RNA in gastric cancer, *Chin. Med. J.*, **133** (2020), 1868–1877.
10. D. Xiong, R. He, Y. Dang, H. Wu, Z. Feng, G. Chen, The latest overview of circRNA in the progression, diagnosis, prognosis and drug resistance of hepatocellular carcinoma, *Front. Oncol.*, **10** (2021), 608257.
11. Y. Li, Q. Zheng, C. Bao, S. Li, W. Guo, J. Zhao, et al., Circular RNA is enriched and stable in exosomes: a promising biomarker for cancer diagnosis, *Cell Res.*, **25** (2015), 981–984.
12. J. Tian, X. Xi, J. Wang, J. Yu, Q. Huang, R. Ma, et al., CircRNA hsa_circ_0004585 as a potential biomarker for colorectal cancer, *Cancer Manage. Res*., **11** (2019), 5413–5423.
13. Z. Li, Z. Chen, G. Hu, Y. Zhang, Y. Feng, Y. Jiang, et al., Profiling and integrated analysis of differentially expressed circRNAs as novel biomarkers for breast cancer, *J. Cell. Physiol.*, **235** (2020), 7945–7959.
14. Y. Zhong, Y. Du, X. Yang, Y. Mo, C. Fan, F. Xiong, et al., Circular RNAs function as ceRNAs to regulate and control human cancer progression, *Mol. Cancer.*, **17** (2018), 79.
15. Z. Dou, L. Gao, W. Ren, H. Zhang, X. Wang, S.Li, et al., CiRS-7 functions as a ceRNA of RAF-1/PIK3CD to promote metastatic progression of oral squamous cell carcinoma via MAPK/AKT signaling pathways, *Exp. Cell Res.*, **396** (2020), 112290.
16. X. Wang, X. Zhu, H. Zhang, S. Wei, Y. Chen, Y. Chen, et al., Increased circular RNA hsa_circ_0012673 acts as a sponge of miR-22 to promote lung adenocarcinoma proliferation, *Biochem. Biophys. Res. Commun.*, **496** (2018), 1069–1075.
17. Z. Sun, Circular RNA hsa_circ_0001588 promotes the malignant progression of lung adenocarcinoma by modulating miR-524-3p/NACC1 signaling, *Life Sci.*, **259** (2020), 118157.

18. L. Liang, L. Zhang, J. Zhang, S. Bai, H. Fu, Identification of circRNA-miRNA-mRNA networks for exploring the fundamental mechanism in lung adenocarcinoma, *Onco Targets Ther.*, **13** (2020), 2945–2955.
19. X. X. Liu, Y. E. Yang, X. Liu, M. Y. Zhang, R. Li, Y. H. Yin, et al., A two-circular RNA signature as a noninvasive diagnostic biomarker for lung adenocarcinoma, *J. Transl. Med.*, **17** (2019), 50.
20. S. Xia, J. Feng, K. Chen, Y. Ma, J. Gong, F. Cai, et al., CSCD: a database for cancer-specific circular RNAs, *Nucleic Acids Res.*, **46** (2018), D925–D929.
21. C. H. Chou, S. Shrestha, C. D. Yang, N. W. Chang, Y. L. Lin, K. W. Liao, et al., miRTarBase update 2018: a resource for experimentally validated microRNA-target interactions, *Nucleic Acids Res.*, **46** (2018), D296–D302.
22. V. Agarwal, G. W. Bell, J. W. Nam, D. P. Bartel, Predicting effective microRNA target sites in mammalian mRNAs, *eLife*, **4** (2015), e05005.
23. P. Shannon, A. Markiel, O. Ozier, N. S. Baliga, J. T. Wang, D. Ramage, et al., Cytoscape: a software environment for integrated models of biomolecular interaction networks, *Genome Res.*, **13** (2003), 2498–2504.
24. D. W. Huang, B. T. Sherman, R. A. Lempicki, Systematic and integrative analysis of large gene lists using DAVID Bioinformatics Resources, *Nat. Protoc.*, **4** (2009), 44–57.
25. D. W. Huang, B. T. Sherman, R. A. Lempicki, Bioinformatics enrichment tools: paths toward the comprehensive functional analysis of large gene lists, *Nucleic Acids Res.*, **37** (2009), 1–13.
26. D. Szklarczyk, A. L. Gable, D. Lyon, A. Junge, S. Wyder, J. Huerta-Cepas, et al., STRING v11: protein-protein association networks with increased coverage, supporting functional discovery in genome-wide experimental datasets, *Nucleic Acids Res.*, **47** (2009), D607–D613.
27. G. D. Bader, C. W. Hogue, An automated method for finding molecular complexes in large protein interaction networks, *BMC Bioinf.*. **4** (2003).
28. Z. Tang, C. Li, B. Kang, G. Gao, C. Li, Z. Zhang, GEPIA: a web server for cancer and normal gene expression profiling and interactive analyses, *Nucleic Acids Res.*, **45** (2017), W98–W102.
29. D. S. Chandrashekar, B. Bashel, S. A. H. Balasubramanya, C. J. Creighton, I. Ponce-Rodriguez, B. V. Chakravarthi, et al., UALCAN: A portal for facilitating tumor subgroup gene expression and survival analyses, *Neoplasia.*, **19** (2017), 649–658.
30. Z. R. Zhou, W. W. Wang, Y. Li, K. R. Jin, X. Y. Wang, Z. W. Wang, et al., In-depth mining of clinical data: the construction of clinical prediction model with R, *Ann. Transl. Med.*, 7 (2019), 796.
31. Y. Zhang, H. Yao, Y. Li, L. Yang, L. Zhang, J. Chen, et al., Circular RNA TADA2A promotes proliferation and migration via modulating of miR-638/KIAA0101 signal in non-small cell lung cancer, *Oncol. Rep.*, **46** (2021), 201.
32. H. Zhao, H. Wei, J. He, D. Wang, W. Li, Y. Wang, et al., Propofol disrupts cell carcinogenesis and aerobic glycolysis by regulating circTADA2A/miR-455-3p/FOXM1 axis in lung cancer, *Cell Cycle*, **19** (2020), 2538–2552.
33. Z. Wu, M. Zheng, Y. Zhang, M. Xie, S. Tian, T. Ding, et al., Hsa_circ_0043278 functions as competitive endogenous RNA to enhance glioblastoma multiforme progression by sponging miR-638, *Aging (Albany NY)*, **12** (2020), 21114–21128.
34. C. Liu, T. Han, Y. Shi, The decreased expression of hsa_circ_0043278 and its relationship with clinicopathological features of breast cancer, *Gland Surg.*, **9** (2020), 2044–2053.

35. F. Tian, C. T. Yu, W. D. Ye, Q. Wang, Cinnamaldehyde induces cell apoptosis mediated by a novel circular RNA hsa_circ_0043256 in non-small cell lung cancer, *Biochem. Biophys. Res. Commun.*, **493** (2017), 1260–1266.
36. Q. Wang, T. Wang, Y. Hu, W. Jiang, C. Lu, W. Zheng, et al., Circ-EIF4G3 promotes the development of gastric cancer by sponging miR-335, *Pathol., Res. Pract.*, **215** (2019), 152507.
37. W. Zhang, Z. Wang, G. Cai, P. Huang, Circ_DOCK1 regulates USP11 through miR-132-3p to control colorectal cancer progression, *World J. Surg. Oncol.*, **19** (2021), 67.
38. L. G. Di, C. M. Croce, miRNA profiling of cancer, *Curr. Opin. Genet. Dev.*, **23** (2013), 3–11.
39. R. Q. He, L. Gao, J. Ma, Z. Y. Li, X. H. Hu, G.Chen, Oncogenic role of miR-183-5p in lung adenocarcinoma: A comprehensive study of qPCR, in vitro experiments and bioinformatic analysis, *Oncol. Rep.*, **40** (2018), 83–100.
40. Y. Lin, Q. Gu, Z. Sun, B. Sheng, C. Qi, B. Liu, et al., Upregulation of miR-3607 promotes lung adenocarcinoma proliferation by suppressing APC expression, *Biomed. Pharmacother.*, **95** (2017), 497–503.
41. Y. L. Wan, H. J. Dai, W. Liu, H. T. Ma, miR-767-3p inhibits growth and migration of lung adenocarcinoma cells by regulating CLDN18, *Oncol. Res.*, **26**(2018), 637–644.
42. X. Wu, T. Liu, O. Fang, W. Dong, F. Zhang, L. Leach, et al., MicroRNA-708-5p acts as a therapeutic agent against metastatic lung cancer, *Oncotarget.*, **7** (2016), 2417–2432.
43. W. Zhou, R. Li, microRNA-605 inhibits the oncogenicity of non-small-cell lung cancer by directly targeting Forkhead Box P1, *Onco Targets Ther.*, **12** (2019), 3765–3777.
44. Y. Wei, Y. Liao, Y. Deng, Y. Zu, B. Zhao, F. Li, MicroRNA-503 inhibits non-small cell lung cancer progression by targeting PDK1/PI3K/AKT pathway, *Onco Targets Ther.*, **12** (2019), 9005–9016.
45. G. Fan, J. Jiao, F. Shen, Q. Ren, Q. Wang, F. Chu, Long non-coding RNA HCG11 sponging miR-522-3p inhibits the tumorigenesis of non-small cell lung cancer by upregulating SOCS5, *Thorac. Cancer.*, **11** (2020), 2877–2886.
46. W. Han, L. Wang, L. Zhang, Y. Wang, Y. Li, Circular RNA circ-RAD23B promotes cell growth and invasion by miR-593-3p/CCND2 and miR-653-5p/TIAM1 pathways in non-small cell lung cancer, *Biochem. Biophys. Res. Commun.*, **510** (2019), 462–466.
47. J. H. Li, S. S. Sun, N. Li, P. Lv, S. Y. Xie, P. Y. Wang, MiR-205 as a promising biomarker in the diagnosis and prognosis of lung cancer, *Oncotarget.*, **8** (2017), 91938–91949.
48. D. B. Mendonça, J. T. Nguyen, F. Haidar, A. L. Fox, C. Ray, H. Amatullah, et al., MicroRNA-1911-3p targets mEAK-7 to suppress mTOR signaling in human lung cancer cells, *Heliyon*, **6** (2020), e05734.
49. B. R. Druliner, J. A. Fincher, B. S. Sexton, D. L. Vera, M. Roche, S. Lyle, et al., Chromatin patterns associated with lung adenocarcinoma progression, *Cell Cycle*, **12** (2013), 1536–43.
50. T. Eguchi, K. Kadota, J. Chaft, B. Evans, J. Kidd, K. S. Tan, et al., Cell cycle progression score is a marker for five-year lung cancer-specific mortality risk in patients with resected stage I lung adenocarcinoma, *Oncotarget*, **7** (2016), 35241–35256.
51. J. Zhu, H. Ao, M. Liu, K. Cao, J. Ma, UBE2T promotes autophagy via the p53/AMPK/mTOR signaling pathway in lung adenocarcinoma, *J. Transl. Med.*, **19** (2021), 374.
52. Y. Tian, X. Tian, X. Han, Y. Chen, C. Y. Song, Y. B. Zhang, et al., Expression of ATP binding cassette E1 enhances viability and invasiveness of lung adenocarcinoma cells in vitro, *Mol. Med. Rep.*, **14** (2016), 1345–50.

53. C. C. Wang, Y. L. Hsu, C. J. Chang, C. J. Wang, T. H. Hsiao, S. H. Pan, Inhibitor of DNA-binding protein 4 suppresses cancer metastasis through the regulation of epithelial mesenchymal transition in lung adenocarcinoma, *Cancers*, **11** (2019), 2021.

AIMS Press